*Mathematical Medicine and Biology* (2013) **30**, 311–337
doi:10.1093/imammb/dqs026
Advance Access publication on September 20, 2012

# Mathematical modelling of cytokine-mediated inflammation in rheumatoid arthritis

Michelle Baker*
*Centre for Mathematical Medicine and Biology, School of Mathematical Sciences, University of Nottingham, Nottingham NG7 2RD, UK*
*Corresponding author: pmxmb2@nottingham.ac.uk

Sarah Denman-Johnson
*School of Mathematics,Loughborough University, Loughborough LE11 3TU, UK*

Bindi S. Brook
*Centre for Mathematical Medicine and Biology, School of Mathematical Sciences, University of Nottingham, Nottingham NG7 2RD, UK*

Ian Gaywood
*Department of Rheumatology, Nottingham University Hospitals NHS Trust, Nottingham, UK*

and

Markus R. Owen
*Centre for Mathematical Medicine and Biology, School of Mathematical Sciences, University of Nottingham, Nottingham NG7 2RD, UK*

[Received on 9 March 2012; revised on 19 June 2012; accepted on 13 August 2012]

Rheumatoid arthritis (RA) is a chronic inflammatory disease preferentially affecting the joints and leading, if untreated, to progressive joint damage and disability. Cytokines, a group of small inducible proteins, which act as intercellular messengers, are key regulators of the inflammation that characterizes RA. They can be classified into pro-inflammatory and anti-inflammatory groups. Numerous cytokines have been implicated in the regulation of RA with complex up and down regulatory interactions. This paper considers a two-variable model for the interactions between pro-inflammatory and anti-inflammatory cytokines, and demonstrates that mathematical modelling may be used to investigate the involvement of cytokines in the disease process. The model displays a range of possible behaviours, such as bistability and oscillations, which are strongly reminiscent of the behaviour of RA e.g. genetic susceptibility and remitting-relapsing disease. We also show that the dose regimen as well as the dose level are important factors in RA treatments.

*Keywords*: ODE; mathematical modelling; cytokines; rheumatoid arthritis; pro-inflammatory; anti-inflammatory.

## 1. Introduction

Rheumatoid arthritis (RA) is a chronic inflammatory joint disease that affects around 1% of the adult population (Witten, 2000). The condition is three times more likely to affect women than men and disease onset generally occurs over the age of 40, although it occurs much earlier in a small number of individuals (Imboden *et al.*, 2007).

The disease is characterized by the chronic inflammation of the synovial lining of joints (synovitis) with consequent destruction of cartilage and bone (Choy & Panayi, 2001). The synovium is a layer of cells lining the joint capsule. In health, this layer is thin and produces small amounts of synovial fluid which nourishes cartilage, reduces friction and absorbs shock. In RA, synovial lining cells proliferate, there is vascular proliferation and the amount of synovial fluid produced increases several fold. Cells in inflammatory synovitis produce high levels of numerous cytokines which act locally to produce the characteristic joint pain, swelling and stiffness, and systemically to produce a range of effects including the production of acute-phase proteins by the liver (Imboden *et al.*, 2007). In addition to being easily measurable markers of inflammation, these proteins contribute to some of the long-term systemic effects of RA including the two-fold increase in cardiovascular mortality (Dhawan & Quyyumi, 2008).

Although it is still not clear what triggers the onset of RA, more is known about the mechanisms of disease progression. RA is an autoimmune disease and once triggered, the synovium is infiltrated with T cells, macrophages and plasma cells (Brennan *et al.*, 1992) which produce cytokines promoting the inflammatory response and leading to tissue destruction (Arend, 2001). In RA, abnormalities in the T cells, including premature telomeric erosion and defects in telomeric repair mechanisms, lead to the loss of normal homoeostatic control of cytokine levels (Goronzy & Weyand, 2009). Telomeres are important chromatin structures at the ends of chromosomes, which protect the DNA from degradation during replication (Blasco, 2005). Studies of RA have shown reductions in telomere length and reduced T cell receptor excision circles, indicating advanced cellular ageing (Koetz *et al.*, 2000).

Cytokines are cell signalling molecules that have many roles within the body. The inflammatory and immune responses are mediated by cytokines, which are raised during periods of inflammation or infection before returning to normal levels. In RA, the chronic nature of the inflammation means that cytokine levels are raised for longer periods and are found systemically as well as at the affected joints. It is thought that cytokine interactions play a crucial role in the development of RA and can modulate the severity and duration of the associated inflammation (Goronzy & Weyand, 2009). Cytokine molecules act as cellular messengers by binding to their specific cell surface-bound receptor molecules. Once bound to an active receptor, a signal is created which alters either the cell function, the type of cytokines it produces or the rate at which it produces them (Arend, 2001). A huge range of cytokines have been identified in the synovium and each one has a unique but overlapping set of functions. They can be classified into pro-inflammatory and anti-inflammatory groups according to the primary function of the cytokine in the synovium. Two of the most important pro-inflammatory cytokines in RA are interleukin-1 (IL-1) and tumour necrosis factor-$\alpha$ (TNF-$\alpha$) (Choy & Panayi, 2001). Examples of anti-inflammatory cytokines found in the synovium include a IL-1 receptor antagonist (IL-1Ra) and IL-10 (Dinarello & Moldawer, 2002). Based on this, we think it is useful to model this system, using the classification of pro- and anti-inflammatory cytokine groups.

Several authors have modelled cytokine-mediated inflammatory processes. Seymour & Henderson (2001) described the behaviour of IL-1 and IL-10, with TNF-$\alpha$ as an external stimulus for IL-1, using a six-variable ODE model. The model showed different types of behaviour including uncontrolled production of IL-1, stable equilibria and stable limit cycles. The authors were able to link the model results to observed behaviour in RA and septic shock. A related model by Jit *et al.* (2005) looked in more depth at only TNF-$\alpha$ and in particular, modelled the effects of anti-TNF-$\alpha$ drugs in the inflamed synovial joint. The study considered the issue of why anti-TNF-$\alpha$ drugs worked well in the treatment of RA but were not effective in Systemic Inflammatory Response Syndrome (SIRS), another TNF-$\alpha$-mediated condition. The authors concluded that cytokine levels in RA were usually in equilibrium and anti-TNF-$\alpha$

forced a shift from a disease equilibrium to a healthy equilibrium, whereas SIRS was a non-equilibrium condition and as such was not able to be moved to a healthy equilibrium state.

A model of acute systemic inflammation as a result of pathogen infection was presented by Kumar *et al.* (2004) and later extended by Reynolds *et al.* (2006). The model identified five possible outcomes dependent on parameters: healthy response, non-infectious inflammation, infectious inflammation, recurrent inflammation and immunodeficient response. A general model of inflammation was proposed by Herald (2010). The model showed that if the macrophage is particularly sensitive to pro-inflammatory cytokines, or if anti-cytokine levels were low, then even small inflammatory responses to infection may become chronic rather than being resolved. To date, there appears to be no RA-specific modelling that considers the dynamics of both pro- and anti-inflammatory cytokines. By modelling these two groups, we can look at the involvement of cytokines in RA onset and treatment, which has not been considered previously.

The redundancy and dual role of many cytokines suggests that a functional rather than chemical classification may prove particularly useful. We therefore aim to represent the complex cytokine network in the synovium by a simple two-variable model. This will allow us to assess whether changes in the parameters governing these two groups and their interactions can lead to the features seen in RA. In addition to looking at the development and progression of RA, we would like to consider the effect of anti-cytokine treatment of RA and consider which properties of treatment lead to a beneficial response.

In the following section, we look at the model development and justify the terms within the model. We also non-dimensionalize the model and give a biological interpretation of each of the parameters. In Section 3 we analyse the model, beginning with consideration of the nullclines and steady states of the system. We then look at bifurcations as we vary the pro-inflammatory cytokine production parameter, which allows us to classify the different types of behaviours in the system. Lastly, we look at bifurcations in two-parameter space and consider how these change for different values of the other three parameters. In Section 4 we consider the possibility of time-dependent changes in patient-specific parameters leading to the onset of RA. In Section 5 we consider the effect of treatment involving doses of pro-inflammatory cytokine inhibitors. We look at different dose levels and regimes and how these affect the behaviour of the model. Finally in Section 6, we consider possible clinical implications of the model as well as its limitations.

## 2. An activator–inhibitor model for cytokine interactions

The synovium consists of a variety of cells including fibroblasts, macrophages and T cells, and each individual cell has a different response pattern (Alberts, 1989). We neglect this variability in cell behaviour and the synovium is modelled as a spatially uniform collection of homogeneous, generic cells. We focus on the cells' production of pro-inflammatory and anti-inflammatory cytokine molecules and neglect other functions such as cytotoxic mechanisms or proliferation. The binding of pro-inflammatory cytokine molecules to membrane-bound receptors induces the production of both pro-inflammatory and anti-inflammatory cytokines while the binding of anti-inflammatory molecules causes a down-regulation in the production of pro-inflammatory molecules. This has been demonstrated by Brennan *et al.* (1992) who showed that TNF-$\alpha$ has both an autocrine and paracrine pro-inflammatory function, and up-regulates itself as well as other pro-inflammatory cytokines (particularly IL-1). TNF-$\alpha$ is also known to up-regulate the production of IL-10, which functions to down-regulate both TNF-$\alpha$ and IL-1 (Dinarello & Moldawer, 2002). IL-10 also up-regulates IL-1Ra, strengthening its anti-inflammatory effect.

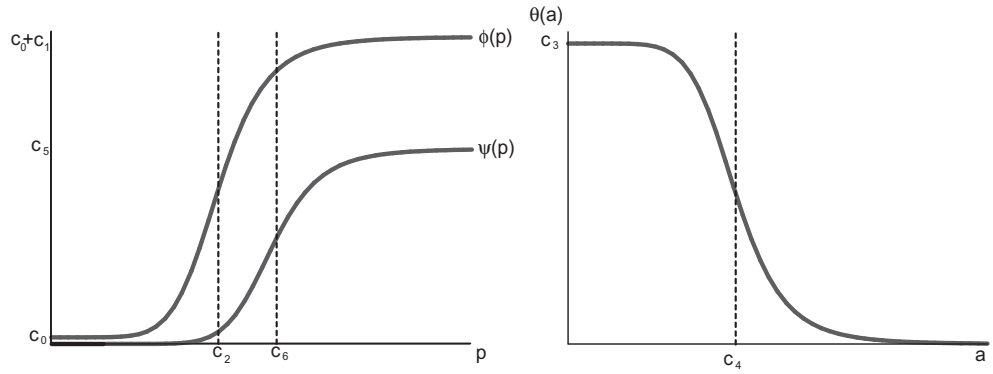


FIG. 1. Examples of qualitative forms for the production feedback functions $\phi(p)$, $\theta(a)$ and $\psi(p)$.

We denote the concentration of pro-inflammatory cytokine molecules by $p$ and the concentration of anti-inflammatory cytokine molecules by $a$. The degradation of a cytokine concentration is assumed to be linear, with rates $d_p$ and $d_a$. The general form of the equations for the cytokine dynamics is then

$$\frac{\mathrm{d}p}{\mathrm{d}t} = -d_p p + \phi(p)\theta(a) \tag{2.1}$$

$$\frac{\mathrm{d}a}{\mathrm{d}t} = -d_a a + \psi(p). \tag{2.2}$$

The product $\phi(p)\theta(a)$ models the combined effect of pro-inflammatory and anti-inflammatory stimuli on pro-inflammatory cytokine production, based on the assumption that anti-inflammatory molecules work by inhibiting the synthesis of pro-inflammatory cytokine molecules (Opal & DePalo, 2000). $\phi(p)$ and $\psi(p)$ are increasing saturating functions of $p$, so that they represent induced up-regulation with some maximum production rate. Similarly, $\theta(a)$ represents the down-regulation of $p$ in response to an increase in $a$ and with a decreasing effect from some maximum at $a = 0$. Examples of functions that have these properties are

$$\phi(p) = c_0 + c_1 \frac{p^{m_1}}{c_2^{m_1} + p^{m_1}}, \quad \theta(a) = c_3 \frac{c_4^{m_2}}{c_4^{m_2} + a^{m_2}} \text{ and } \psi(p) = c_5 \frac{p^{m_3}}{c_6^{m_3} + p^{m_3}},$$

where $c_0, c_1, c_2, c_3, c_4, c_5$ and $c_6$ are non-negative constant parameters. Since pro-inflammatory production is stimulated by an external stimulus, a background production term $c_0$ has been included in $\phi(p)$, anti-inflammatory production is stimulated only by pro-inflammatory cytokine molecules and so no background term is necessary. The coefficients $m_1$, $m_2$ and $m_3$ will all be taken as 2 for the analysis of this system since values greater than 2 show qualitatively similar behaviour and a value of 1 reduces the range of behaviours, this is discussed further in Appendix A. Some sample forms for these feedback functions are shown in Fig. 1. The model equations are non-dimensionalized using

$$p = p^* c_2, \quad a = a^* c_4 \quad \text{and} \quad t = t^* \frac{1}{d_a}.$$

TABLE 1 *Summary of the dimensionless parameters in the cytokine dynamics model* (2.3–2.4)

| Parameter | Interpretation |
|---|---|
| $\alpha_1$ | Background pro-inflammatory production rate |
| $\alpha_2$ | Magnitude of additional pro-inflammatory cytokine production |
| $\alpha_3$ | Pro-inflammatory cytokine concentration at which anti-inflammatory production is half maximal |
| $\alpha_4$ | Magnitude of anti-inflammatory cytokine production |
| $\gamma$ | Relative rate of clearance of pro-inflammatory cytokine to anti-inflammatory cytokine |

With the asterisks dropped for notational simplicity and setting $m_1 = m_2 = m_3 = 2$, (2.1–2.2), with the equations for $\phi$, $\theta$ and $\psi$, become

$$\frac{\mathrm{d}p}{\mathrm{d}t} = -\gamma p + \frac{1}{1+a^2}\left(\alpha_1 + \alpha_2 \frac{p^2}{1+p^2}\right) \tag{2.3}$$

$$\frac{\mathrm{d}a}{\mathrm{d}t} = -a + \alpha_4 \frac{p^2}{\alpha_3^2 + p^2}, \tag{2.4}$$

where

$$\alpha_1 = \frac{c_0 c_3}{c_2 d_a}, \quad \alpha_2 = \frac{c_1 c_3}{c_2 d_a}, \quad \alpha_3 = \frac{c_6}{c_2}, \quad \alpha_4 = \frac{c_5}{c_4 d_a} \text{ and } \gamma = \frac{d_p}{d_a}.$$

The parameter $\alpha_1$ is the background production rate for pro-inflammatory cytokine so that when $a = p = 0$, pro-inflammatory production occurs at a rate of $\alpha_1$. The parameter $\alpha_2$ corresponds to the maximum rate of pro-inflammatory cytokine production over and above the basal rate. $\alpha_3$ is the concentration of pro-inflammatory cytokines at which anti-inflammatory production is half maximal. $\alpha_4$ corresponds to the maximum rate of production of anti-inflammatory cytokine. Here, $\gamma$ is the ratio of the rate of pro-inflammatory and anti-inflammatory decay. The significance of these parameters is summarized for reference in Table 1 and appropriate values for these parameters are discussed in Appendix B.

In the following sections we will show how bistability and oscillatory behaviour can arise from this model and consider possible interpretations of this behaviour in a biological context.

## 3. Model analysis

### 3.1 *Nullclines and steady states*

To analyse the steady states of this system, we will consider the forms of the nullclines, and consider only the positive quadrant. The nullclines of the system (2.4), (2.3) respectively, are as follows:

$$a = N_1(p) = \frac{\alpha_4 p^2}{\alpha_3 + p^2}$$

$$a = N_2(p) = \sqrt{f(p)},$$

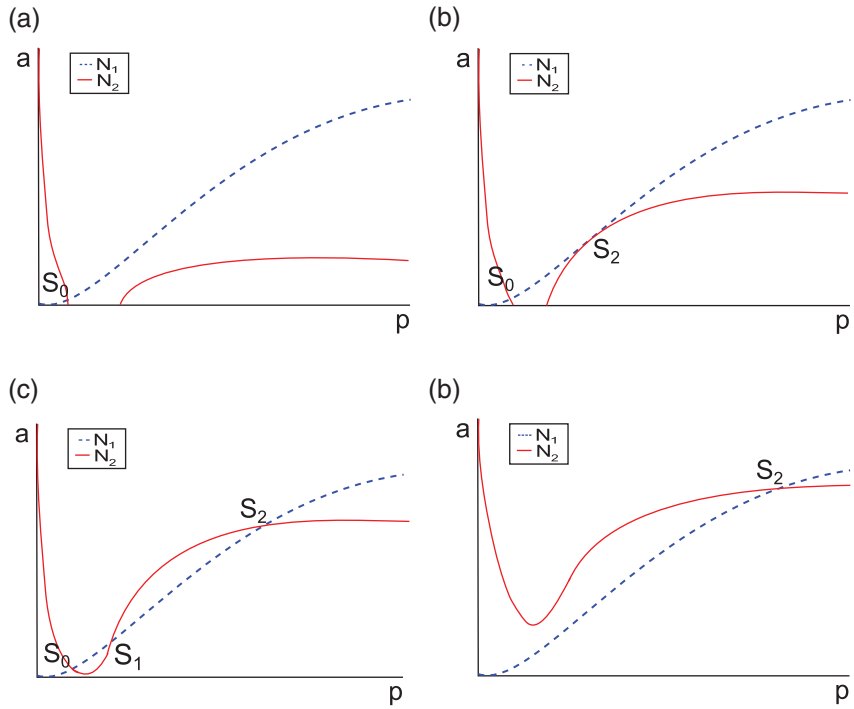


FIG. 2. Schematic showing the nullclines of the system (2.3), (2.4) and the different ways they may intersect when $\alpha_2 > 8\alpha_1$. The dashed line represents the $a$ nullcline ($\mathrm{d}a/\mathrm{d}t = 0$) and the solid line represents the $p$ nullcline ($\mathrm{d}p/\mathrm{d}t = 0$).

where

$$f(p) = \frac{p^2(\alpha_1 + \alpha_2) + \alpha_1}{\gamma p(1 + p^2)} - 1.$$

Figure 2 shows the ways that these nullclines may intersect and hence how the steady states may arise. It is clear from this diagram that there is always at least one steady state and for some parameter values three steady states exist.

Analysis of the turning points of the nullclines (Appendix C) tells us that, when $\alpha_2 < 8\alpha_1$ there can only be one steady state, and when $\alpha_2 > 8\alpha_1$ there is either one, two or three steady states (see Fig. 2). The case of two state states only occurs when the nullclines touch but do not cross and as such only exists for an extremely narrow set of parameters. For this reason, throughout this paper, we will only consider the one and three steady state cases. The steady states are denoted $S_0$, $S_1$ and $S_2$. Where they exist, $S_0$ is stable, $S_1$ is unstable and $S_2$ can be either stable or unstable (Appendix C).

### 3.2 *One parameter bifurcation diagrams*

Of the five free parameters, the cytokine production rates ($\alpha_2$ and $\alpha_4$) are rates that change as part of the immune response and so are likely to change over time in response to injury or therapeutic intervention. If we assume that the rate of clearance is determined by the size and structure of the cytokine and by the

TABLE 2 *Summary of the behaviour types in the cytokine dynamics model* (2.3–2.4)

| Case | Steady states | Limit cycles |
|---|---|---|
| Ai | $S_0$: stable | — |
| Aii | $S_2$: stable | — |
| Aiii | $S_0$: stable; $S_1$: unstable; $S_2$: unstable | — |
| B | $S_2$: unstable | $L_1$: stable |
| Ci | $S_0$: stable; $S_1$: unstable; $S_2$: stable | — |
| Cii | $S_0$ stable; $S_1$ unstable; $S_2$: stable | $L_2$: unstable |
| Di | $S_0$: stable; $S_1$: unstable; $S_2$: unstable | $L_1$: stable |
| Dii | $S_0$: stable; $S_1$: unstable; $S_2$: unstable | $L_1$: stable; $L_2$: unstable |

chemical environment within the host, it is reasonable to assume that the decay rate parameter $\gamma$ will remain constant in an individual (or vary over a much longer timescale than that over which cytokine interactions occur). Similarly, we assume that the background production rate and the anti-inflammatory production threshold parameter, $\alpha_1$ and $\alpha_3$, respectively, are fixed within an individual. To demonstrate the types of behaviour that can arise from this model, we consider bifurcation diagrams of variations in $\alpha_2$ for a range of different values of the other parameters. The types of behaviour displayed are summarized in Table 2 and discussed in detail below. All bifurcation plots and simulations in this paper were produced in XPPAUT (Ermentrout, 2002).

3.2.1 *Monostable and bistable behaviour.* In a simple case, illustrated in Fig. 3, two-fold bifurcations give rise to monostable and bistable behaviour. For sufficiently small values of $\alpha_2$, monostable behaviour is seen where trajectories undergo at most one peak in $p$ before decaying to the steady state $S_0$, which has a low level of $p$ (case Ai). The phase plane for this case is shown in Fig. 3(b), and the nullclines correspond to Fig. 2(a). This case could generally be considered as a healthy state since $p$ is always low and there are no oscillations.

For intermediate values of $\alpha_2$, bistable behaviour is observed, with two stable steady states and a single unstable steady state (case Ci), shown in Fig. 3(c). In this case, the stable manifold of $S_1$ divides the phase space into two regions: the basin of attractions of the healthy state $S_0$ and of the disease state $S_2$. The values of $\alpha_2$ and $\alpha_4$ determine the size of the region contained within the stable manifold. Increasing $\alpha_4$ decreases the size of the region, whereas increasing $\alpha_2$ increases the size of the region. This means that if anti-inflammatory production is increased, then the set of disease states is smaller, and if the pro-inflammatory production is increased, the set of disease states is larger. One counter-intuitive observation to be made from Fig. 3(c) is that any state within the disease region could be returned to the healthy state by a stimulus that increases the pro-inflammatory concentration sufficiently. This would cause a further increase in $p$, triggering an anti-inflammatory response, which would raise both $a$ and $p$ before returning both to lower levels at the healthy steady state. Similarly, but more intuitively, a sufficient increase in the anti-inflammatory concentration can always return the system to a state of health.

Finally, for sufficiently large $\alpha_2$ there is another monostable case (case Aii), in which all trajectories in the phase plane undergo oscillations of decaying magnitude to $S_2$ (Fig. 3(d)). In this case, the value of $p$ is generally relatively high, indicative of a disease state. However, as $\alpha_4$ is increased the value of $p$ at $S_2$ decreases, and case Aii starts to behave like case Ai, making the distinction between health and disease less clear. Changes in $\alpha_4$ are discussed further in Section 3.3.

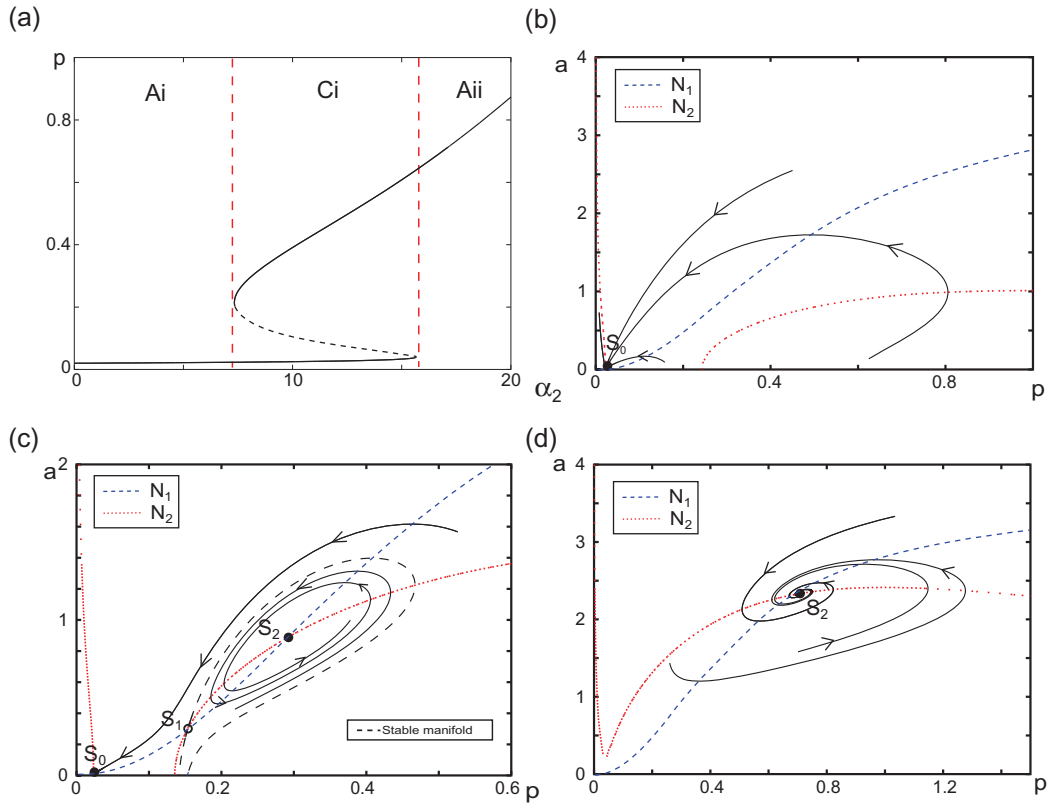


FIG. 3. Monostable and bistable behaviour in the model (2.3–2.4) for the interaction between pro- and anti-inflammatory cytokines ($\alpha_1 = 0.025, \alpha_3 = 0.5, \alpha_4 = 3.5$ and $\gamma = 1.25$). (a) The bifurcation plot of $p$ against $\alpha_2$. The solid lines represent stable branches while the dashed lines represent unstable branches. The vertical dashed lines signify the thresholds between different behaviour types. (b) The phase plane plot of Case Ai, a single healthy steady state ($\alpha_2 = 5$). (c) The phase plane plot of Case Ci, two stable steady states ($S_0$ and $S_2$) and one unstable steady state ($S_1$) ($\alpha_2$ = 8). (d) The phase plane plot of Case Aii, a single unhealthy steady state with ($\alpha_2 = 17$).

3.2.2 *Monostable and bistable behaviour with oscillations.* For larger values of $\alpha_4$ (approximately three-fold increase compared with Fig. 3(a)), the model also displays oscillatory behaviour in addition to the behaviours described in Section 3.2.1 (Fig. 4). This more complex bifurcation diagram corresponds to two additional types of phase-plane behaviour. The first type, case Di, has a single stable steady state ($S_0$), two unstable steady states ($S_1$ and $S_2$) and a stable limit cycle around $S_2$ (Fig. 4(b)). In this situation the limit cycle represents inflammation in the system due to fluctuating high levels of $p$ (perhaps reflecting relapsing-remitting disease). This case is similar to Ci, with all states within the stable manifold of $S_1$, evolving to the disease limit cycle and all states outside evolving to the healthy state.

The second new behaviour, case B, has only a single unstable steady state ($S_2$) surrounded by a stable limit cycle (Fig. 4(c)). The limit cycle can be thought of as a disease state due both to high levels of $p$ and the oscillatory behaviour. This is similar to case Aii, since all trajectories undergo decaying oscillations into the disease limit cycle.

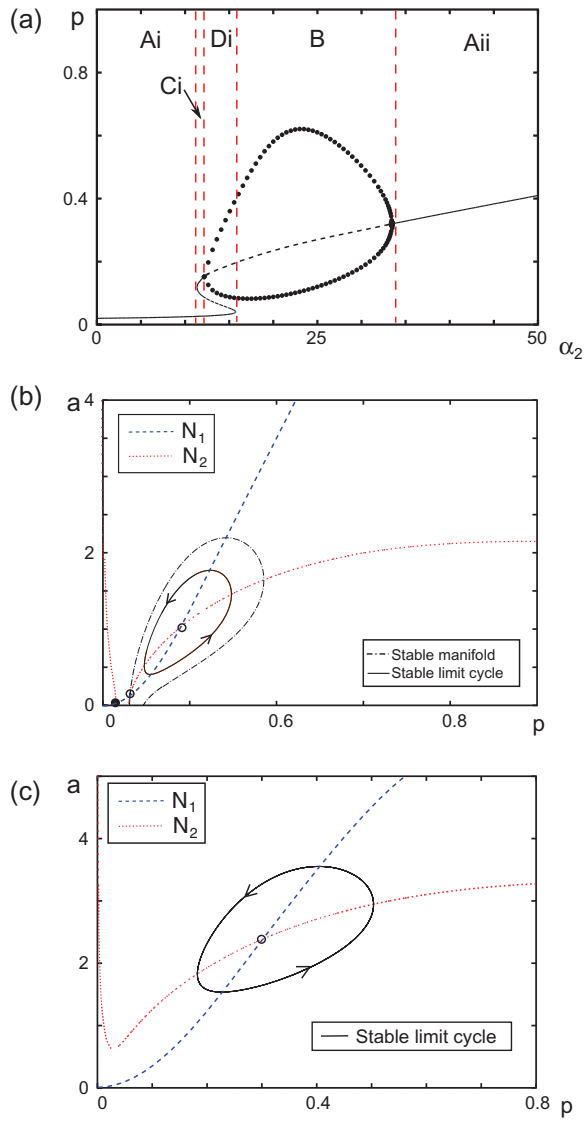


FIG. 4. Monostable and bistable behaviour with oscillations in the model (2.3–2.4) for the interaction between pro- and anti-inflammatory cytokines ($\alpha_1 = 0.025, \alpha_3 = 0.5, \alpha_4 = 9$ and $\gamma = 1.25$). (a) The bifurcation plot of $p$ against $\alpha_2$. The solid lines represent stable branches, whereas the dashed lines represent unstable branches. The vertical dashed lines signify the thresholds between different behaviour types. (b) The phase plane plot of Case Di, one stable steady state ($S_0$), two unstable steady states and a stable limit cycle around $S_2$ ($\alpha_2 = 15$). (c) The phase plane plot of Case B, one unstable steady state ($S_2$) surrounded by a globally stable limit cycle ($\alpha_2 = 30$). Cases Ai, Ci and Aii are shown in Fig. 3.

The bifurcation plot in Fig. 4(a) shows that as $\alpha_2$ is increased, it goes through a fold bifurcation, then a Hopf, followed by a second fold and finally a second Hopf. For larger values of $\alpha_4$ (approximately six-fold increase compared with Fig. 3(a)), we encounter both the folds before the Hopf bifurcations

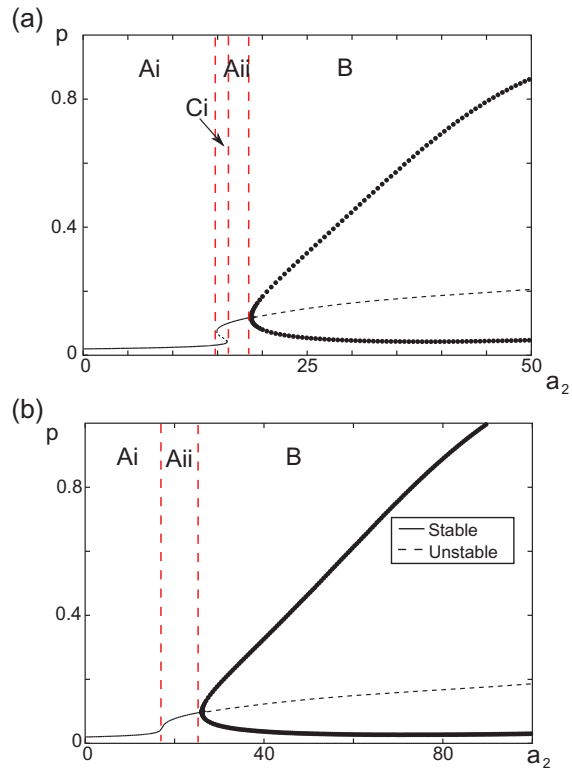


FIG. 5. Bifurcation plots for different values of $\alpha_4$ showing how cases Ci and Di are lost compared with Fig. 4(a) ($\alpha_1 = 0.025, \alpha_3 = 0.5$ and $\gamma = 1.25$) The solid lines represent stable branches, whereas the dashed lines represent unstable branches. The vertical dashed lines signify the thresholds between different behaviour types. (a) $\alpha_4 = 18$, first Hopf bifurcation moves to right of the second fold and case Di (b) $\alpha_4 = 30$, folds coalesce and all bistability is lost.

(Fig. 5(a)), which means that we lose Di behaviour. As $\alpha_4$ is increased further, (approximately 10-fold increase compared with Fig. 3(a)) Ci behaviour is also lost (Fig. 5(b)).

3.2.3 *Monostable and bistable behaviour with homoclinic bifurcations.* For a small range of parameters, there is a saddle node bifurcation that gives rise to a stable limit cycle, $L_1$, surrounded by an unstable limit cycle, $L_2$ (Fig. 6(a)). There is also a homoclinic bifurcation where the unstable limit cycle $L_2$ collides with the steady state $S_1$, giving rise to additional behaviours. A monostable region exists with a stable steady state $S_0$ and two unstable steady states, $S_1$ and $S_2$ (case Aiii). This case behaves similarly to Ai, except that within the stable manifold trajectories will approach $S_0$ in an oscillatory manner (Fig. 6(b)). For a very narrow parameter range, the system is bistable (Fig. 6(c)) with one stable steady state and one stable limit cycle, as well as two unstable steady states and an unstable limit cycle (case Dii). The stable limit cycle $L_1$ with high pro-inflammatory cytokine concentrations, represents a disease state and lies inside the unstable cycle, $L_2$. Here $L_2$ defines the basin of attraction of the disease cycle and the most suitable treatment strategy depends on the current stage in the cycle. For example, if an individual has a high level of $a$ and an intermediate level of $p$, then to bring about a state of health,

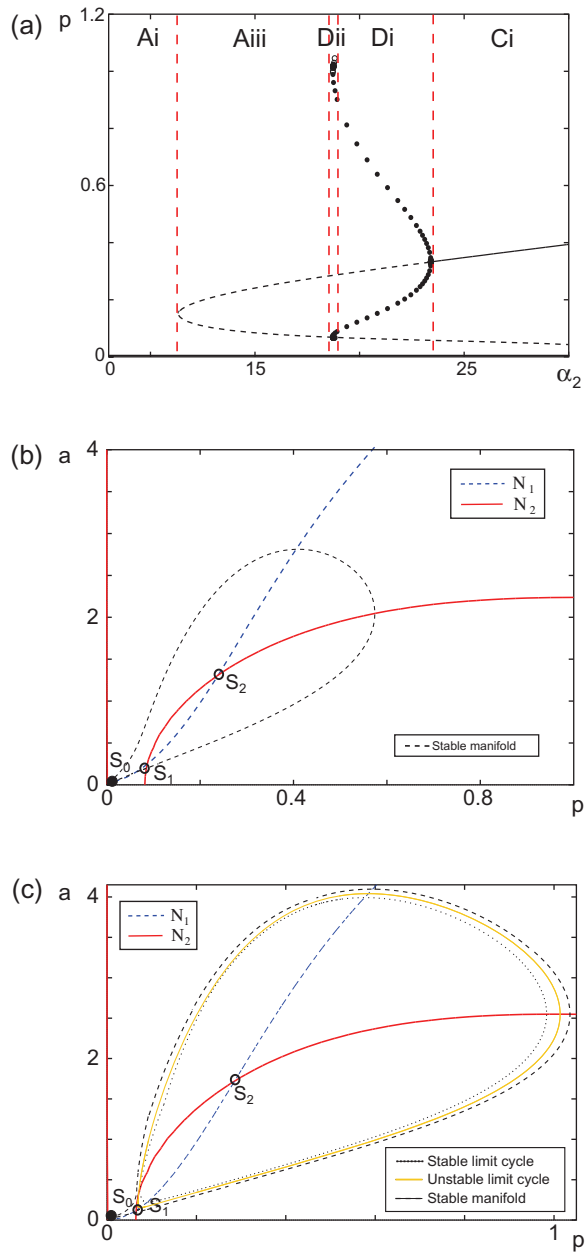


FIG. 6. Monostable and bistable behaviour with homoclinic bifurcations in the model (2.3–2.4) for the interaction between pro- and anti-inflammatory cytokines, showing the new behaviours Aiii and Dii. (a) The bifurcation plot of $\alpha_2$ against $p$. The solid lines represent stable branches, whereas the dashed lines represent unstable branches. The vertical dashed lines signify the thresholds between different behaviour types. (b) The phase plane plot of Case Aiii, a stable steady state ($S_0$) and two unstable steady states ($\alpha_2$ = 15). (c) The phase plane plot of Case Dii, a stable steady state ($S_0$), two unstable steady states, a stable limit cycle and an unstable limit cycle ($\alpha_2$ = 18.73). Cases Ai, Ci and Di are shown in Fig. 4. ($\alpha_1 = 0, \alpha_3 = 0.5, \alpha_4 = 7$ and $\gamma = 1.25$).

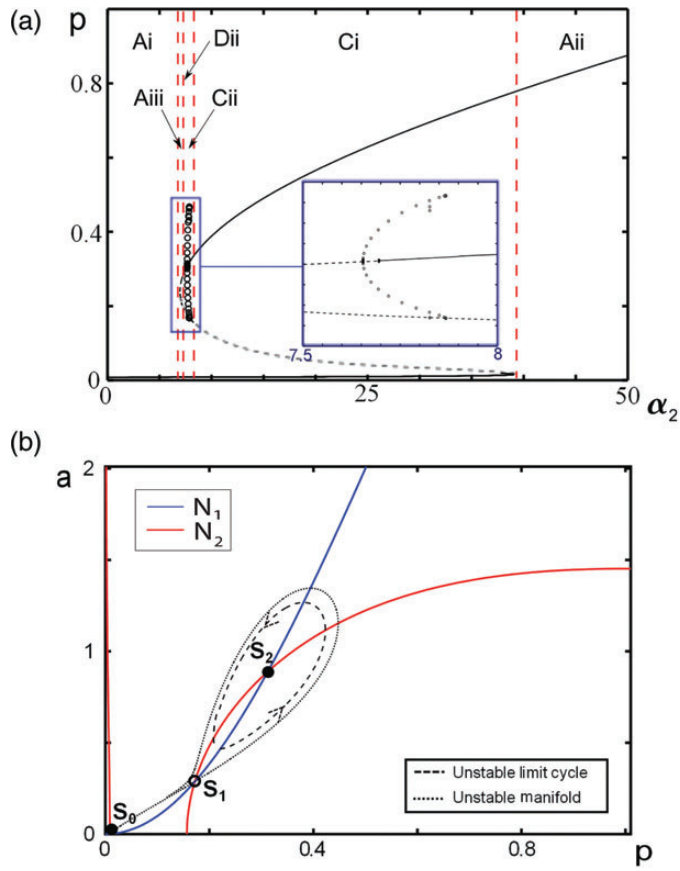


FIG. 7. Bistable behaviour with a homoclinic bifurcation in the model (2.3–2.4) for the interaction between pro and anti-inflammatory cytokines. (a) Bifurcation plot showing $\alpha_2$ plotted against $p$. The inset shows how Case Cii arises through a supercritical Hopf bifurcation where the branch of limit cycles turns and becomes unstable almost immediately after bifurcation. The solid lines represent stable branches whilst the dashed lines represent unstable branches. The vertical dashed lines signify the thresholds between different behaviour types. (b) Phase plane plot showing case Cii, two stable steady states ($S_0$ and $S_2$), an unstable state($S_1$) and an unstable limit cycle around $S_2$ ($\alpha_2 = 7.75$). Cases Ai, Aii, Aiii and Ci are shown in Figs 4 and 6. ($\alpha_1 = 0.01$, $\alpha_3 = 1$, $\alpha_4 = 10$ and $\gamma = 1.25$).

an increase in anti-inflammatory cytokine would be more effective than a decrease in pro-inflammatory cytokine of similar magnitude.

3.2.4 *Bistable behaviour with a homoclinic bifurcation.* One final type of behaviour (case Cii) can be seen for larger values of $\alpha_3$ (Fig. 7). Here, an unstable limit cycle exists with two stable steady states ($S_0$ and $S_2$) and one unstable steady state ($S_1$). The limit cycle is the boundary of the basin of attraction of $S_2$. The unstable manifold of $S_1$ divides the remaining region into those states which evolve to health in an oscillatory fashion (those inside the unstable manifold) and those which have at most one extremum (those outside the unstable manifold). This state arises though a supercritical Hopf bifurcation, where the branch of limit cycles turn and become unstable almost immediately after the bifurcation.

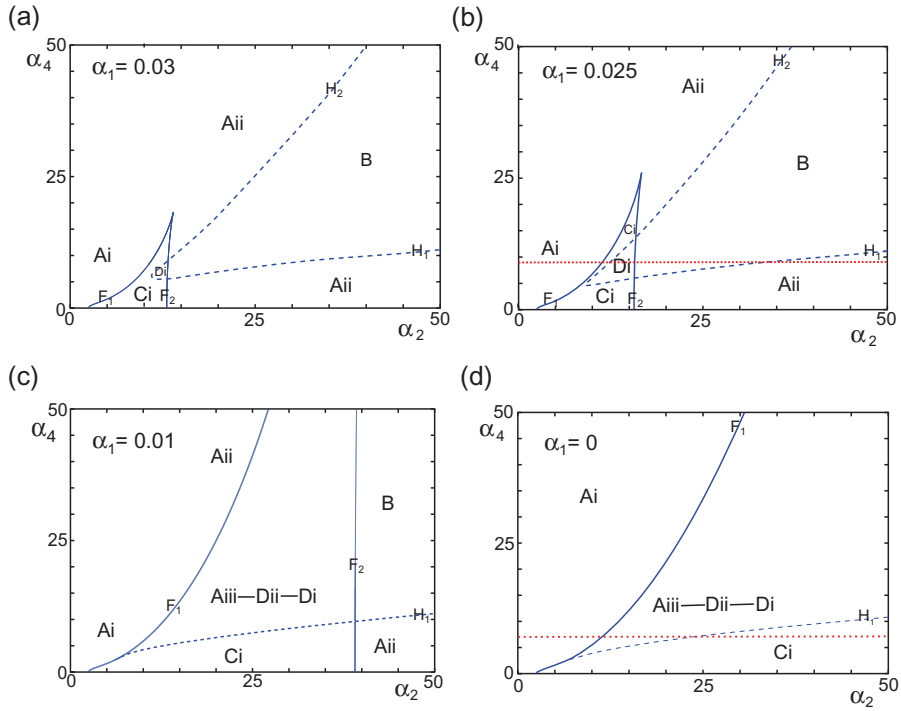


FIG. 8. Parameter space plots in $\alpha_2$–$\alpha_4$ ($\alpha_3 = 0.5$ and $\gamma = 1.25$) showing the fold ($F_1$ and $F_2$) and Hopf ($H_1$ and $H_2$) bifurcations and types of the phase space for decreasing values of $\alpha_1$.(a) Cases Ai, Aii, B, Ci and Di are shown. (b) Cases Ai, Aii, B, Ci and Di are shown. The horizontal dashed line represents a slice through the parameter space at $\alpha_4 = 9$, consistent with the bifurcation plot in Fig. 4 ($\alpha_1 = 0.025$). (c) Cases Ai, Aii, Aiii, B, Ci, Di and Dii are shown., (d) Cases Ai, Aii, Aiii, Ci, Di and Dii are shown. The horizontal dashed line represents a slice through the parameter space at $\alpha_4 = 7$, consistent with the bifurcation plot in Fig. 6 ($\alpha_1 = 0$).

So far we have considered only variations in the pro-inflammatory cytokine production rate $\alpha_2$. It is likely that the anti-inflammatory cytokine production rate $\alpha_4$ is also important in determining disease activity since anti-inflammatory cytokines will mitigate the pro-inflammatory cytokine response. Hence, in the next section we will look at the $\alpha_2$–$\alpha_4$ parameter space for different values of the other three parameters.

### 3.3 *Two-parameter bifurcation diagrams*

In Section 3.2 we examine qualitative changes in the bifurcation structure as $\alpha_4$ varies. It is useful to consider the two-parameter bifurcation structure in the $\alpha_2$–$\alpha_4$ parameter space. Figure 8 shows two-parameter bifurcation diagrams for several different values of $\alpha_1$. It illustrates the curves of Hopf and fold bifurcation points and the types of phase-plane behaviour that are observed in this space and demonstrates the effect that changes in $\alpha_1$ have on the bifurcations. The Hopf bifurcations are denoted by $H_1$ and $H_2$, and the fold bifurcations are denoted by $F_1$ and $F_2$. The dotted line in Fig. 8(b) represents the one-parameter bifurcation diagram shown in Fig. 4. It is now clear why increasing $\alpha_4$ results in the loss of Di and Ci, since the overlap of the regions enclosed by the Hopf and fold bifurcations is decreased and then the folds are destroyed at the cusp. It is important to make the distinction between a healthy

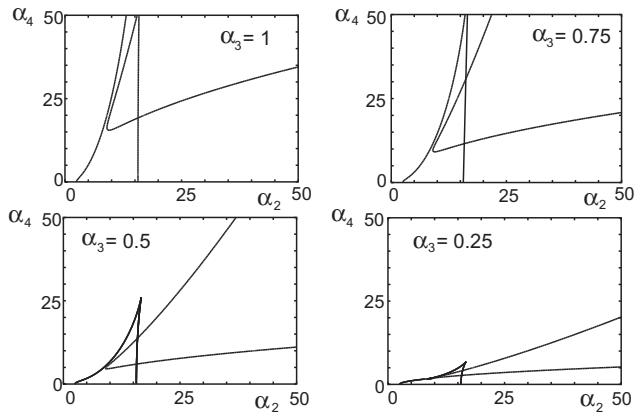


FIG. 9. Figure showing the dependence on threshold parameter $\alpha_3$ of the location of fold and Hopf bifurcations in the $\alpha_2$–$\alpha_4$ parameter space for parameter values ($\alpha_1 = 0.025$, $\gamma = 1.25$).

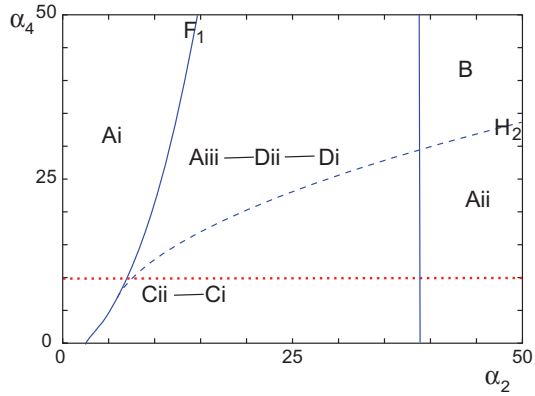


FIG. 10. The $\alpha_2$–$\alpha_4$ parameter space showing all cases. The horizontal dashed line represents a slice through the parameter space at $\alpha_4 = 10$, consistent with the bifurcation plot in Fig. 7 ($\alpha_1 = 0.01, \alpha_3 = 1$ and $\gamma = 1.25$).

state and a disease state since, when $\alpha_4$ is sufficiently small, there is a range of $\alpha_2$ over which two observable stable steady states can coexist. Where there are two stable steady states, the relative levels of $p$ allow one to be designated as disease and the other as health, since in any individual baseline levels of cytokines may vary. Where there is only only stable state, designation of health or disease is more difficult.

As $\alpha_1$ is decreased, one of the Hopf bifurcations is lost and the cusp where the fold bifurcations meet occurs at larger values of both $\alpha_2$ and $\alpha_4$. The background production parameter $\alpha_1$ does not significantly alter the position of the Hopf bifurcation $H_1$. However, as $\alpha_1$ is decreased, $H_2$ moves closer to $F_1$, with $H_2$ eventually being destroyed, leaving the system with only one Hopf bifurcation, $H_1$, which is then supercritical as before and can cause the creation of a stable limit cycle (and for a small range of parameters an unstable one as well).

Figure 8(d) shows the two-parameter bifurcation diagram for $\alpha_1 = 0$. When $\alpha_1 = 0$ and there is no background production, the steady-state structure of the system changes. Since there is no background

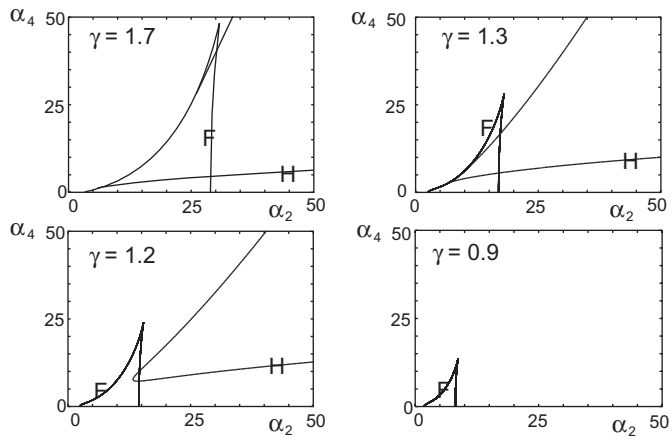


FIG. 11. Diagrams showing the positions of the fold (F) and Hopf (H) bifurcations in the $\alpha_2$–$\alpha_4$ parameter space for decreasing values of $\gamma$ and the parameters ($\alpha_1 = 0.025$ and $\alpha_3 = 0.5$).

production, when the system is at zero concentration, no cytokine can be produced and it must remain at this state, thus the healthy state $S_0$ is fixed at ($p = 0, a = 0$) and is stable. The system still has an unstable state $S_1$ and a state $S_2$ which can be stable or unstable. Since $S_2$ occurs at a relatively high value of $p$, if $S_2$ is stable it can represent a disease state with either no limit cycle or an unstable limit cycle. $S_2$ can also be unstable with either no limit cycle (in which case the system can only be in the healthy cytokine-free state) or a stable limit cycle (with the system in either the healthy state or in a state of periodically varying cytokine concentrations). When this is compared with the behaviour when $\alpha_1 > 0$, we see that cases Aii and B are no longer possible since there is always a stable healthy state.

Variations in $\alpha_3$ and $\gamma$ show similar effects to variations in $\alpha_1$. Figure 9 shows $\alpha_2$–$\alpha_4$ parameter space diagrams for a range of values of $\alpha_3$. As $\alpha_3$ increases, the cusp at which the fold bifurcations meet and are destroyed occurs for a higher value of anti-inflammatory production parameter $\alpha_4$. The pro-inflammatory production parameter $\alpha_2$ at the cusp varies little with $\alpha_3$. One consequence of this effect is that if the threshold $\alpha_3$ is large, then the range of states which can exhibit health and disease is increased. When $\alpha_3$ is small, most conditions lead to the case where there is a single state with pro- and anti-inflammatory concentrations varying according to $\alpha_2$. Figure 10 shows a two-parameter bifurcation diagram for a large value of $\alpha_3$ but a smaller value of $\alpha_1$. Here, all the possible behaviours are observed through variations in $\alpha_2$ and $\alpha_4$.

Figure 11 shows $\alpha_2$–$\alpha_4$ parameter space diagrams for various values of $\gamma$ and demonstrates that as $\gamma$ decreases, the fold and Hopf bifurcations move apart. This means that the parameter region over which there is bistability decreases and the majority of parameter space leads to a single generic stable steady state or a stable limit cycle.

## 4. Time-dependent parameter variations

Some cases of RA have a characteristic mode of onset in which an initially healthy individual experiences flaring and remitting inflammation (palindromic RA) over a sustained length of time before eventually reaching a state of persistent synovitis. The model given by (2.3–2.4) is capable of reproducing some of the key features of this onset pattern by using a time-dependent pro-inflammatory

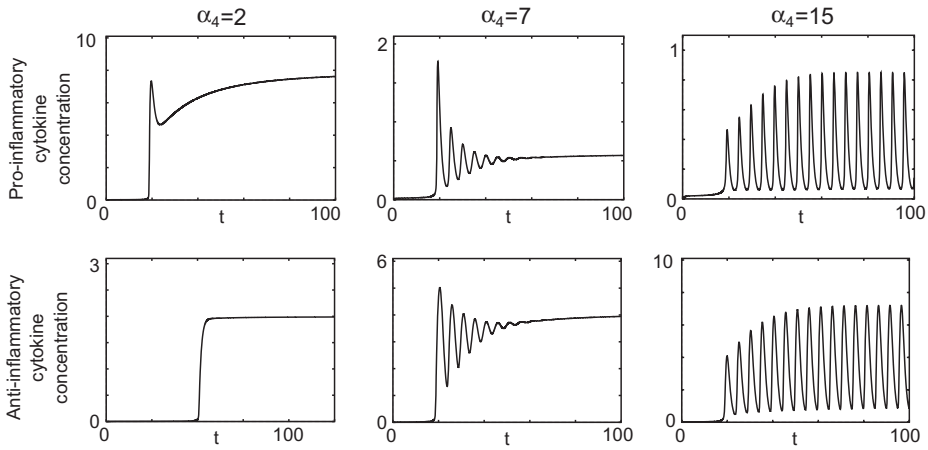


FIG. 12. Plots of pro-inflammatory and anti-inflammatory cytokine concentrations for $\alpha_4$ = 2, 7 and 15. ($\alpha_1 = 0.025$, $\alpha_3 = 0.5$, $\gamma = 1.25$). In each case, the system moves to a disease state over time as $\alpha_2$ increases. As $\alpha_4$ gets larger, the time the system is in an oscillatory state increases until, for some value of $\alpha_4$, the system moves onto a stable limit cycle. The parameter $\alpha_2$ increases over time and this is equivalent to taking a horizontal slice through the bifurcation diagram in Fig. 8(b).

production parameter $\alpha_2$. It is likely that such fluctuations in $\alpha_2$ occur *in vivo* due either to a spontaneous rise in pro-inflammatory cytokine production in response to injury or infection or a gradual rise in production with increasing age (Csiszar *et al.*, 2003; Roubenoff *et al.*, 1998). To illustrate the potential of this approach, we can consider $\alpha_2$ as an increasing, saturating function of time,

$$\alpha_2(t) = a_2^{\min} + \frac{(a_2^{\max} - a_2^{\min})t^2}{a_2^{T\,2} + t^2}$$

so that $\alpha_2(0) = a_2^{\min}$ with $\alpha_2$ increasing with time and $\lim_{t\to\infty} \alpha_2(t) = a_2^{\max}$. The parameter $a_2^T$ is the time at which the $\alpha_2(t)$ is at half maximal. We take $a_2^{\min} = 1$, $a_2^{\max} = 50$ and $a_2^T = 15$ with the remaining parameters assuming the values $\{\gamma = 1.25,\ \alpha_1 = 0.025,\ \alpha_3 = 0.50\}$.

Simulations are run for a set of constant values of $\alpha_4$, equivalent to taking a horizonal section through the parameter plane in Fig. 8(b). It is immediately obvious that $\alpha_4$ will be critical in determining the evolution pattern. To show this effect, the simulation is run for the values $\alpha_4 = \{2, 7, 15\}$ and the concentration evolution in each case is shown in Fig. 12.

These results show that in each case, when $\alpha_2$ is sufficiently large, the system is forced to the disease state $S_2$ but significant differences in the form of the cytokine response are observed. For low $\alpha_4$, as $\alpha_2$ increases, the state is forced to go up to stable disease without any oscillations. For larger $\alpha_4$, as $\alpha_2$ increases, the state is still forced into stable disease but has an intermediate period of oscillations. The length of time over which the system is in an oscillatory state increases with $\alpha_4$ and, for a large $\alpha_4$, the system is forced into sustained oscillations. The highest values of $\alpha_4$ result in a disease state with lowest pro-inflammatory concentration and highest anti-inflammatory concentration. These concentration patterns emphasize the differences which can be attributed to an individual's ability to produce anti-inflammatory cytokines. Those individuals with a faster rate of anti-inflammatory cytokine production (large $\alpha_4$) may be more likely to see the remitting and relapsing pattern of disease onset.

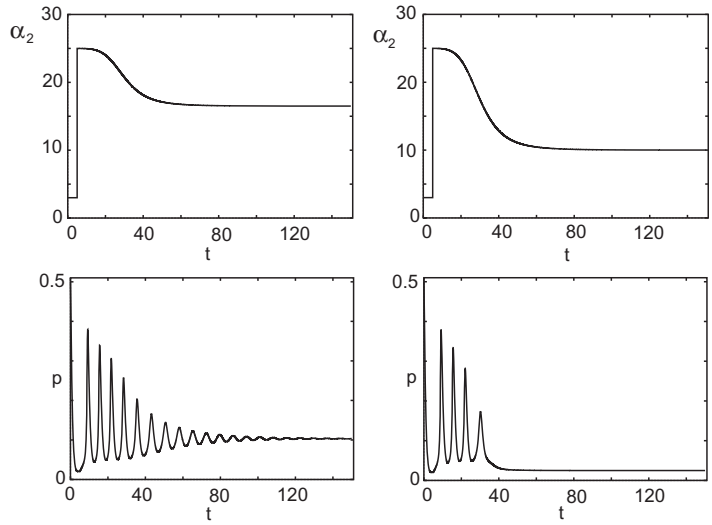


FIG. 13. Plots of $\alpha_2$ and pro-inflammatory cytokine concentrations against time . The two plots in the upper panel show two forms of the $\alpha_2$ function; in both cases $\alpha_2$ starts at 3 and spikes to 25 after $t = 5$. They then settle to a new value of $\alpha_2$, 16.5 in the first column and 10 in the second. The plots in the lower panel show how the concentration of pro-inflammatory cytokine varies over the same time period. Both plots show decaying oscillations to a steady state; in the first column the steady state is a disease state and in the second it is healthy.

The function used here for $\alpha_2$ is representative of an age-related gradual increase in $\alpha_2$ over time. Responses due to infection may lead to an initial spike in pro-inflammatory cytokine production rate ($\alpha_2$) followed by the gradual decline of the rate to a new baseline rate (Fig. 13). In this case the system may settle either to a state of health or disease, determined by the value of $\alpha_2$ after infection. For appropriate parameter values, there may be a period of oscillations, which may be representative of the mechanism by which some individuals go on to develop sustained RA after a period of palindromic RA, while others move into remission.

## 5. Treatment strategies

Some individuals with RA are treated with doses of pro-inflammatory cytokine inhibitors, known as anti-cytokine therapy, either in the form of pro-inflammatory cytokine receptor antagonists or antibodies targeting pro-inflammatory cytokines (Goldbach-Mansky & Lipsky, 2003). Doses are given either by subcutaneous injection or intravenous infusion at intervals ranging from weekly to four-weekly. Short-term effects of the reduction of pro-inflammatory cytokine activity include reduction in joint swelling, pain and stiffness and improvement in general well-being. Long-term effects include reduction in the rate and severity of joint damage. For simplicity, we assume that each dose of pro-inflammatory cytokine inhibitors causes a proportional decrease in the pro-inflammatory cytokine level. We then use an instantaneous decrease in pro-inflammatory cytokine concentration ($p$) in the model to mimic these cytokine treatments. Some effects similar to those reported during cytokine treatment, such as a temporary reduction in disease activity or remission, are exhibited by the model.

To see the importance of the dose size and the interval, parameters for which the system displays type Ci behaviour (see Section 3.2.1) are taken so that the system can show both healthy and disease

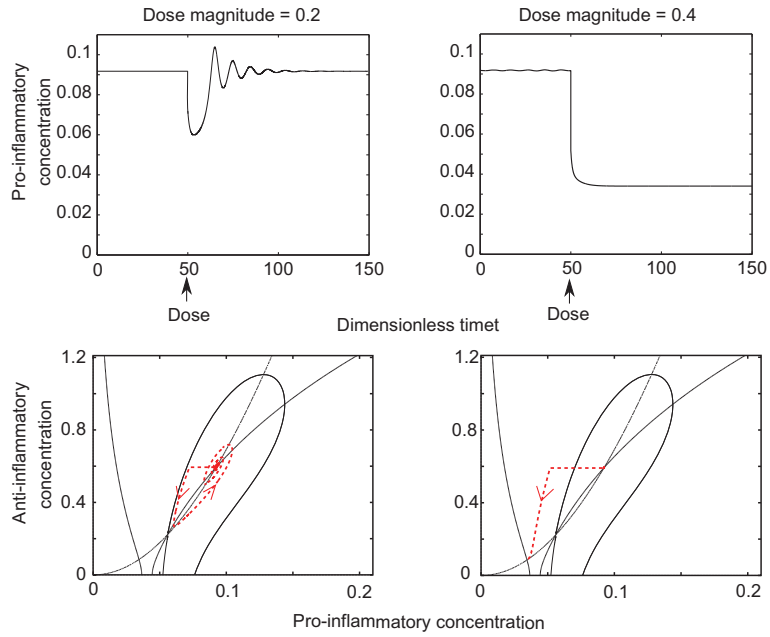


FIG. 14. The pro-inflammatory and anti-inflammatory cytokine concentration response to a single infusion of anti-inflammatory cytokine at time $t = 50$ (dose of magnitude 0.20 in the first column and 0.40 in the second). The time courses of the anti-inflammatory cytokine concentration are not shown for brevity, but profiles look similar to the pro-inflammatory cytokine concentration. The parameters used are $\{\alpha_1 = 0.025,\ \alpha_2 = 15.5,\ \alpha_3 = 0.5,\ \alpha_4 = 18$ and $\gamma = 1.25\}$.

stable steady states. We start the system at a stable disease state ($S_2$) and reduce the value of $p$ by a fixed amount at a specific time point. An increase in dose magnitude indicates an increase in the size of the reduction in the level of $p$. If the system is at the disease state and a single dose of anti-cytokine treatment is given, then the response of the system depends entirely on the size of that dose.

A reduction in the pro-inflammatory concentration which is not sufficient to shift the system to a state outside the basin of attraction of $S_2$ can cause a temporary fall in the pro-inflammatory concentration followed by an overshoot and decaying oscillations back to the disease state (Fig. 14). A larger dose can be sufficient to trigger a monotonic decrease in $p$ until the system settles at the healthy state. This is not a feature that is normally seen in clinical practice, which may suggest that either the dose levels used do not move the system outside of the basin of attraction of $S_2$, or that disease relapses by a change in the parameters, moving the system from a healthy steady state.

The pattern of treatment is also pivotal to the results obtained. By administering multiple treatments, it may be possible to achieve results which are not seen for a single dose, although the timing can be crucial. Using the same parameter values as in Fig. 14, taking a dose of magnitude 0.2 (which as a single dose did not return the system to $S_0$) and giving two doses at different intervals shows that the response depends in a non-trivial way on timing (Fig. 15).

A dose interval at 10 units drives the system to the stable healthy state, while a 15-unit interval sees a return to stable disease after an initial response. Remarkably, a longer interval can be beneficial, for a 17-unit interval a healthy state is achieved. This dependence on timing arises because in the second dosing interval protocol, the second dose is applied when the pro-inflammatory and

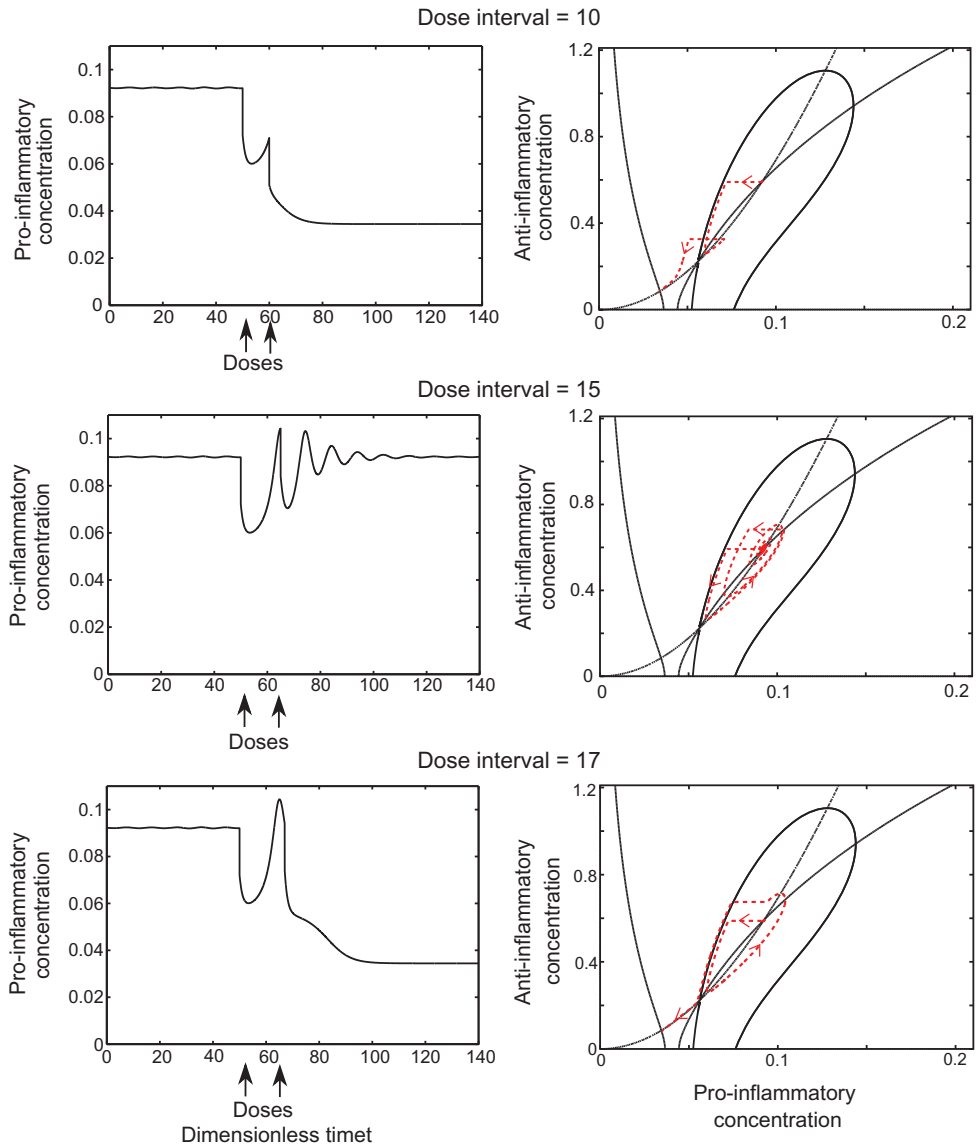


FIG. 15. Time dependence of the pro-inflammatory and anti-inflammatory cytokine concentration for different time separation between doses. All doses have a magnitude of 0.2 and the parameters values are $\{\alpha_1 = 0.025,\ \alpha_2 = 15.5,\ \alpha_3 = 0.5,\ \alpha_4 = 18$ and $\gamma = 1.25\}$. The first row shows the time courses of the pro-inflammatory concentration for two doses given 10, 15 and 17 time units apart. The time courses of the anti-inflammatory cytokine concentration are not shown for brevity, but profiles look similar to the pro-inflammatory cytokine concentration. The second row shows the phase plane diagrams of the simulations.

anti-inflammatory concentration have risen significantly from their first minimum, meaning that the second dose is insufficient to force the trajectory out of the stable manifold (Fig. 15). In the first and third cases, the second dose is administered at the point where the pro-inflammatory concentration is

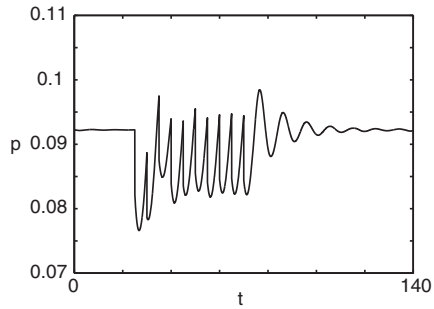


FIG. 16. The pro-inflammatory cytokine profile for the system with doses of anti-inflammatory cytokine of magnitude 0.1 at 5 unit intervals between $t = 25$ and $t = 75$ and parameters $\{\alpha_1 = 0.025,\ \alpha_2 = 15.5,\ \alpha_3 = 0.5,\ \alpha_4 = 18$ and $\gamma = 1.25\}$.

low and so pushes the trajectory out of the basin of attraction of the disease state. The trajectory must be sufficiently close to the basin boundary (the manifold) at the time the second dose is given.

So far, each of the doses provided has been able to shift the system to the healthy state. Some doses, however, are not large enough to achieve this, regardless of the number of doses unless the pattern of dose administration is changed. Using the same parameters as before with a dose size of half the previous smallest dose (0.1) and applying it at time intervals of 5 units over a sustained period of time, we obtain the pro-inflammatory concentration profile shown in Fig. 16. This treatment pattern brings about a temporary reduction in the concentration of pro-inflammatory cytokines although there are oscillations in the level. When the treatment ceases, the pro-inflammatory cytokine concentration returns to the pretreatment level. Only by reducing the time interval can this change be sustained after treatment has ceased.

## 6. Discussion

### 6.1 *Cytokines are important mediators in RA*

The success of clinical treatments based on altering the synovial cytokine profile suggests that the composition and interactions of the cytokine network are key factors in at least the regulation, if not the onset, of RA (Feldmann & Maini, 2001). The model developed here is a two-variable activator-inhibitor system that simulates the dynamics of two classes of cytokines, pro-inflammatory and anti-inflammatory. Five key dimensionless parameters have been identified. We have shown that the model can have either one steady state ($S_0$ or $S_2$) or three steady states ($S_0$, $S_1$ and $S_2$). This leads to a range of a phase plane behaviours.

### 6.2 *Monostable and bistable behaviour*

The model shows four types of monostable phase plane behaviour (Ai, Aii, Aiii and B). These behaviours may be interpreted as a healthy response (Ai and Aiii) due to a low level of $p$, a disease response due to a high level of $p$ (B) or an unclear response of health/disease due to an intermediate range of $p$. In addition to monostable behaviour, the model also shows four types of bistable phase plane behaviour (Ci, Cii, Di and Dii). These have a stable healthy steady state and a stable disease state which is either a fixed point or a limit cycle. One point to note is that if an individual has a high level of pro-inflammatory production, so that a monostable disease state prevails, increasing the magnitude of anti-inflammatory production, $\alpha_4$, does not return the system to distinct health, but does reduce the

level of $p$ at the fixed point (see Fig. 8(b)). In clinical practice, only cytokine concentrations are changed rather than production rates, and so increasing the magnitude of anti-inflammatory cytokine production would relate only to intrinsic changes in rates at present. However, this may be relevant for development of gene therapy approaches.

### 6.3 *Time-dependent parameter changes and the onset of disease*

Figure 12 shows that as the pro-inflammatory production parameter ($\alpha_2$) increases over time, the system moves from the healthy steady state to a disease state. Here, the anti-inflammatory production parameter $\alpha_4$ determines the pattern of disease onset. As $\alpha_4$ increases, the approach to the disease state changes from a straightforward switch to an oscillatory one. The size of $\alpha_4$ determines the time taken for the oscillations to settle until, for some larger $\alpha_4$, we have sustained oscillations. These counter-intuitive features highlight the need for a well-defined measure of the link between the cytokine profile and synovial inflammation in the model, since lower cytokine levels may still result in a longer period of persistent disease. Figure 13 shows that temporary spikes in the pro-inflammatory production parameter, which may represent a response to infection, can also initiate the onset of disease. In this case, the onset of disease is determined by the level of pro-inflammatory cytokine production after the initial spike.

### 6.4 *Dose interval and size are crucial for anti-cytokine treatment*

Cytokine treatment simulations show the relevance of the dose size to the efficacy of a particular treatment. Two doses were applied when the system was at rest at the disease state (Fig. 14). We demonstrated that the larger dose could move the system to a state of health, while the smaller dose was insufficient. If multiple doses were given the smaller dose could be used to move the system to health; however, the dose interval used here is crucial. The key factor in determining the dose interval is the point in the oscillatory cycle at which the second or subsequent dose is administered (Fig. 15). Intuitively, the best time to apply the second dose is when the pro-inflammatory concentration is at its lowest so that the cumulative effect is as large as possible. Mathematically, the best time to apply it is when the horizontal separation in the ($p$, $a$) phase plane between the bounding curve of the basin of attraction of $S_2$ and the concentration trajectory is at a minimum, since this gives the best chance of leaving the basin of attraction of the disease state. These conditions are not necessarily equivalent. If the side effects of a high dose of a drug are unacceptable, then we have shown that it may be possible to apply a course of smaller doses at targeted times to return the system to health. Clearly, it may be possible to manipulate the treatment regime to include the smallest possible dose over the fewest possible applications. The model has the surprising property that an increase in the pro-inflammatory cytokine level can also bring about remission; this has not been tested clinically but has interesting implications for novel treatment strategies.

### 6.5 *Anti-cytokine treatment is beneficial even where remission is not possible*

In parameter regimes where only the disease state exists, no treatment of the types described here, no matter how large the dose, could ever achieve remission (i.e. a sustained state of health). Manipulation of the system parameters is the only way this could be achieved. However, a dose of anti-cytokine therapy would move an individual to a lower pro-inflammatory cytokine level temporarily followed by a gradual return to the disease state. This is still a desirable outcome in clinical practice and justifies the use of anti-cytokine therapy, particularly when given as a series of regular treatments, even where remission is impossible.

### 6.6 *Window of opportunity for remission corresponds with regions of bistability*

We believe that a healthy individual at a low risk of developing RA will have parameters corresponding to a phase plane with a single, globally stable, steady state. Individuals with very early RA or at a high risk of developing RA will have parameters defining a system with three steady states. These individuals may go on to occupy a steady disease state from which it is possible to return to a healthy state by appropriate manipulation of pro- and anti-inflammatory cytokine levels. Correspondingly, clinicians refer to a window of opportunity in treating early RA during which remission is more likely than in later disease, implying the time dependence of the underlying parameters. In clinical practice, the closure of this window of opportunity marks the transition from early to established disease. In this model, it may mark the transition from a system with three steady states to one with a single, steady, inescapable disease state characterized by high pro-inflammatory cytokine levels, which occurs as $\alpha_2$ changes. In established RA, remission rates with anti-cytokine therapy, even when combined with other types of immunosuppression, are only around 20%, suggesting that the majority of patients with established RA are in this state.

### 6.7 *Interpretation and outlook*

This model has produced many of the features observed in real cytokine systems, but if the characteristics of this model are to be interpreted in a clinical context, then it is necessary to link the concentration of cytokines to a measurable disease indicator. Ideally, we would like to link the model results to clinical data of cytokine levels over time in individuals with early and late RA. Practical considerations, including the short half-life of cytokines and the difficulty of extracting synovial fluid from the joint, indicate that this type of data is difficult to obtain in humans. It may be possible to collect similar data from animal models or, alternatively, we may be able to use other types of clinical data. The inflammatory marker C-reactive protein (CRP) is routinely used by clinicians as a measure of disease activity in RA. However, the variation between individuals is large and the link between the cytokine level and CRP level or inflammation is as yet unclear. That said, in the majority of cases we identify from our model, the interpretation is very clear. We either have low levels of $p$ indicating health or high levels of $p$ indicating disease. It is only when the levels are intermediate that we are unable to define a clear threshold between health and disease. While there is no precise link between model variables and specific disease markers, the interactions in the model are well established and the predictions are robust to variations in parameter values and functional forms. It would ultimately be desirable to have a model that includes a number of specific cytokines and measurable disease markers to allow a clear link between model behaviour and disease activity. This would give us a better idea of how cytokine levels influence disease manifestations and would provide a clearer definition of health and disease.

## Funding

This research was supported by Industrial CASE Partnership Grant BB/I532353/1 from the Biotechnology and Biological Sciences Research Council (BBSRC) and Pfizer.

## References

Alberts, B. (1989) *Molecular Biology of the Cell*. New York: Garland Publishing.
Arend, W. P. (2001) Physiology of cytokine pathways in rheumatoid arthritis. *Arthritis Care Res.*, **45**, 101–106.
Blasco, M. A. (2005) Telomeres and human disease: ageing, cancer and beyond. *Nat. Rev. Genet.*, **6**, 611–622.

Brennan, F. M., Maini, R. N. & Feldmann, M. (1992) TNF-$\alpha$—a pivotal role in rheumatoid arthritis? *Rheumatology*, **31**, 293–298.

Choy, E. H. S. & Panayi, G. S. (2001) Cytokine pathways and joint inflammation in rheumatoid arthritis. *N. Engl. J. Med.*, **344**, 907–916.

Csiszar, A., Ungvari, Z., Koller, A., Edwards, J. G. & Kaley, G. (2003) Aging-induced pro-inflammatory shift in cytokine expression profile in coronary arteries. *FASEB J.*, **17**, 1183–1185.

Dhawan, S. & Quyyumi, A. (2008) Rheumatoid arthritis and cardiovascular disease. *Curr. Atheroscler. Rep.*, **10**, 128–133.

Dinarello, C. A. & Moldawer, L. L. (2002) *Pro-inflammatory and Anti-inflammatory Cytokines in Rheumatoid Arthritis*, 2nd edn. USA: Amgen Inc.

Ermentrout, B. (2002) *Simulating, Analyzing, and Animating Dynamical Systems: A Guide to Xppaut for Researchers and Students*. Philadelphia: Society for Industrial and Applied Mathematics.

Feldmann, M. & Maini, R. N. (2001) Anti-TNF$\alpha$ therapy of rheumatoid arthritis: what have we learned? *Annu. Rev. Immunol.*, **19**, 163–196.

Goldbach-Mansky, R. & Lipsky, P. E. (2003) New concepts in the treatment of rheumatoid arthritis. *Annu. Rev. Med.*, **54**, 197–216.

Goronzy, J. & Weyand, C. (2009) Developments in the scientific understanding of rheumatoid arthritis. *Arthritis Res. Ther.*, **11**, 1–14.

Herald, M. (2010) General model of inflammation. *Bull. Math. Biol.*, **72**, 765–779.

Imboden, J. B., Stone, J. H. & Hellmann, D. B. (2007) *Current Rheumatology Diagnosis & Treatment*. New York, NY: Lange Medical Books/McGraw-Hill, Medical Pub. Division.

Jit, M., Henderson, B., Stevens, M. & Seymour, R. M. (2005) TNF$-\alpha$ neutralization in cytokine-driven diseases: a mathematical model to account for therapeutic success in rheumatoid arthritis but therapeutic failure in systemic inflammatory response syndrome. *Rheumatology*, **44**, 323–331.

Koetz, K., Bryl, E., Spickschen, K., O'Fallon, W. M., Goronzy, J. J. & Weyand, C. M. (2000) T cell homeostasis in patients with rheumatoid arthritis. *Proc. Natl Acad. Sci.*, **97**, 9203–9208.

Kumar, R., Clermont, G., Vodovotz, Y. & Chow, C. C. (2004) The dynamics of acute inflammation. *J Theor Biol*, **230**, 145–155.

Opal, S. M. & DePalo, V. A. (2000) Anti-inflammatory cytokines. *Chest*, **117**, 1162–1172.

Reynolds, A., Rubin, J., Clermont, G., Day, J., Vodovotz, Y. & Bard Ermentrout, G. (2006) A reduced mathematical model of the acute inflammatory response: I. Derivation of model and analysis of anti-inflammation. *J. Theor. Biol.*, **242**, 220–236.

Roubenoff, R., Harris, T. B., Abad, L. W., Wilson, P. W. F., Dallal, G. E. & Dinarello, C. A. (1998) Monocyte cytokine production in an elderly population: effect of age and inflammation. *J. Gerontol. A Biol. Sci. Med. Sci.*, **53A**, M20–M26.

Seymour, R. M. & Henderson, B. (2001) Pro-inflammatory—anti-inflammatory cytokine dynamics mediated by cytokine-receptor dynamics in monocytes. *Math. Med. Biol.*, **18**, 159–192.

Witten, T. (2000) Modeling the progression of articular erosion in rheumatoid arthritis (RA): initial mathematical models. *Math. Comput. Model.*, **31**, 31–38.

## Appendix A. Hill coefficients

So far we have taken all the Hill coefficients ($m_1$, $m_2$ and $m_3$) to be 2. In this section, we will justify this choice by examining some other possibilities and considering the effect these would have on the model.

$$\frac{\mathrm{d}p}{\mathrm{d}t} = -\gamma p + \frac{1}{1+a^{m_2}}\left(\alpha_1 + \alpha_2 \frac{p^{m_1}}{1+p^{m_1}}\right) \tag{A.1}$$

$$\frac{\mathrm{d}a}{\mathrm{d}t} = -a + \alpha_4 \frac{p^{m_3}}{\alpha_3 + p^{m_3}}. \tag{A.2}$$

The Hill coefficients from the functions $\phi(p)$ $\psi(p)$ and $\theta(a)$ also appear in the non-dimensionalized equations in the form of (A.1–A.2). There are three main alternatives to the assumption we have made; firstly that all the coefficients are the same but are some value greater than 2; secondly that all the coefficients are 1 or finally that we have some combination of different coefficients for the different terms in the model.

### A.1 *Hill coefficients* $m_1, m_2, m_3 > 2$

For coefficients greater than 2 the qualitative shape of the Hill function does not change; only its steepness does. This means that, for $m_1, m_2, m_3 > 2$, the nullclines of the system will cross in a similar manner, and we expect qualitatively similar behaviour, with the stability of the steady states and the types of bifurcations unchanged. The only change we would expect is alterations in the values of parameters at which the various bifurcations occur.

### A.2 *Hill coefficient* $m_1 = m_2 = m_3 = 1$

Since the shape of the Hill function when the coefficient is 1 is different from when it is greater than 1, the behaviour of the model is also likely to change. In this situation, the model equations become

$$\frac{\mathrm{d}p}{\mathrm{d}t} = -\gamma p + \frac{1}{1+a}\left(\alpha_1 + \alpha_2 \frac{p}{1+p}\right), \tag{A.3}$$

$$\frac{\mathrm{d}a}{\mathrm{d}t} = -a + \alpha_4 \frac{p}{\alpha_3 + p}, \tag{A.4}$$

which gives the nullclines

$$a = N_1(p) = \frac{\alpha_4 p}{\alpha_3 + p}$$

$$a = N_2(p) = \frac{p(\alpha_1 + \alpha_2) + \alpha_1}{\gamma p(1+p)} - 1.$$

As in the original model, $N_1$ is monotonically increasing. However, now $N_2$ is monotonically decreasing in $p$ and hence there can be no more than a single steady state.

### A.3 *Mixed Hill coefficients*

So far we have only considered situations where all three Hill coefficients are $\geqslant 2$ or equal to 1, but the coefficients are independent and could have different values. Since values greater than 2 behave the same as a value of 2, we only need to consider combinations of 1 and 2. Also, if we look at the nullcline $N_1$, it is a monotonically increasing function regardless of the value of $m_3$, and so we need only look at two situations: $m_1 = 2, m_2 = m_3 = 1$ and $m_1 = 1, m_2 = 2, m_3 = 1$.

In the first case, when $m_1 = 2, m_2 = m_3 = 1$, $N_2$ becomes

$$a = N_2(p) = \frac{p^2(\alpha_1 + \alpha_2) + \alpha_1}{\gamma p(1+p^2)} - 1.$$

This is the same as $f(p)$ in Appendix C and has two real, positive turning points, meaning that we can have either one or three steady states. This exhibits similar behaviour to the original model except that the steady states tend to occur at larger values of both $p$ and $a$.

In the second case, when $m_1 = 1$, $m_2 = 2$ and $m_3 = 1$, $N_2$ becomes

$$a = N_2(p) = \sqrt{f(p)},$$

where

$$f(p) = \frac{p(\alpha_1 + \alpha_2) + \alpha_1}{\gamma p(1+p)} - 1.$$

Here $f(p)$ is monotonically decreasing, so that $N_2$ must also be monotonically decreasing in the positive quadrant, and can cross $N_1$ only once, giving exactly one steady state. This situation is similar to the case when all the coefficients are 1 and exhibits similar behaviour. Essentially, $m_1$ must be greater than 1 to give bifurcations and bistability in the model i.e. strong feedback in $p$ is required.

## Appendix B. Parameter values

Throughout this work we explore the behaviour of the system by looking at different parameter values and so it is useful to have some idea of the values that would be reasonable. We can gain some insight into this by examining the definitions of the parameters.

We define by $\gamma = d_p/d_a$ the relative rate of clearance and it is the ratio of the pro-inflammatory to anti-inflammatory cytokine degradation rates. If we assume that these degradation rates are likely to be similar, then we would expect $\gamma$ to be close to 1.

We denote by $\alpha_3$ the ratio of the $EC_{50}$ of the anti-inflammatory production to the $EC_{50}$ of the pro-inflammatory production. Since we require anti-inflammatory molecules to down-regulate the pro-inflammatory response, we would expect these to have reasonably similar values, and hence we would expect $\alpha_3$ to be of order 1.

We denote by $\alpha_2$ the maximum pro-inflammatory cytokine production rate and we would expect this to be of the same order as the maximum anti-inflammatory cytokine production rate $\alpha_4$. Through numerical analysis and examination of the nullclines, we can see that if $\alpha_2$ and $\alpha_4$ are of a greater order of magnitude than the other model parameters, the model only has a single unstable steady state with a stable limit cycle, indicative of disease. Since this is unlikely to be representative of either healthy individuals or RA individuals, we will consider parameter values for $\alpha_2$ and $\alpha_4$ of order 1, similar to the other parameters, which allows a greater range of behaviours.

We denote by $\alpha_1$ the background level of pro-inflammatory cytokine production. To have an effective response to infection and injury, the background level of cytokines must be much smaller than the event stimulated production, and hence $\alpha_1$ needs to be small, and should be much smaller than $\alpha_2$.

It has not been possible to obtain more accurate parameter values from the literature, since we are not able to measure these rates *in vivo* and there is no appropriate *in vitro* data for RA. However, this work in ongoing and we hope to be able to produce better parameter estimates from experimental data in the future.

## Appendix C. Number and stability of steady states

The nullclines of the system (2.4), (2.3), respectively, are as follows:

$$a = N_1(p) = \frac{\alpha_4 p^2}{\alpha_3 + p^2}$$
$$a = N_2(p) = \sqrt{f(p)},$$

where

$$f(p) = \frac{p^2(\alpha_1 + \alpha_2) + \alpha_1}{\gamma p(1 + p^2)} - 1.$$

We cannot find the steady states of this system analytically but, by looking at the turning points of each nullcline, we can identify how many possible steady states there may be. Here $N_1(p)$ is simply an increasing Hill function and hence has no turning points and always goes through the point $(p, a) = (0, 0)$. The number of turning points of $N_2(p)$ cannot be found analytically but since we need only consider real positive values of $p$ and $a$, we can see that the number of turning points of $N_2(p)$ will be equal to the number of turning points in $f(p)$.

Differentiating $f(p)$ shows that it has four possible turning points (C.1), (C.2).

$$p = \frac{\sqrt{2}}{2} \frac{\sqrt{(\alpha_1 + \alpha_2)((\alpha_2 - 2\alpha_1) \pm \sqrt{{\alpha_2}^2 - 8\alpha_2\alpha_1)}}}{\alpha_1 + \alpha_2} \tag{C.1}$$

$$p = -\frac{\sqrt{2}}{2} \frac{\sqrt{(\alpha_1 + \alpha_2)((\alpha_2 - 2\alpha_1) \pm \sqrt{{\alpha_2}^2 - 8\alpha_2\alpha_1)}}}{\alpha_1 + \alpha_2}. \tag{C.2}$$

We see that $p$ will always be either negative or complex in (C.2), leaving only two possible turning points. If $\alpha_2 < 8\alpha_1$, then both these points will be complex. This means that $N_2$ will be a monotonically decreasing function and will cross $N_1$ only once, giving a single steady state. Otherwise, $f(p)$ and consequently $N_2$ will have two turning points and so will cross $N_1$ three times, giving a maximum of three steady states. It is not possible to find the stability of the steady states analytically, but the Jacobian $A$, shown below, does give us some information regarding the stability:

$$A = \begin{pmatrix} -\gamma + \dfrac{2\alpha_2}{(1+a^2)} \dfrac{p}{(1+p^2)^2} & \dfrac{-2a}{(1+a^2)^2} \left(\alpha_1 + \alpha_2 \dfrac{p^2}{1+p^2}\right) \\ 2\alpha_4 \dfrac{\alpha 3^2 p}{({\alpha_3}^2 + p^2)^2} & -1 \end{pmatrix}.$$

From this the trace and the determinant of the system are, respectively,

$$\text{Trace}\, A = \frac{2\alpha_2}{(1+a^2)} \frac{p}{(1+p^2)^2} - \gamma - 1 \tag{C.3}$$

$$\text{Det}\, A = \gamma - \frac{2\alpha_2}{(1+a^2)} \frac{p}{(1+p^2)^2} + 4\alpha_4 \frac{a}{1+a^2} \left(\alpha_1 + \alpha_2 \frac{p^2}{1+p^2}\right) \left(\frac{p}{{\alpha_3}^2 + p^2} - \frac{p^3}{({\alpha_3}^2 + p^2)^2}\right). \tag{C.4}$$

We can see that when $p \ll 1$ and $a \ll 1$, then $\text{Trace}\, A \approx -\gamma - 1$ and $\text{Det}\, A \approx \gamma$, and so, for a small $p$ and $a$, $S_0$ will be stable. At some point, for steady states at larger values of $p$ and $a$, the steady state loses

stability. For very large values of $p$, $\mathrm{Trace}\,A \approx -\gamma - 1$ and $\mathrm{Det}\,A \approx \gamma$; so $S_2$ is stable for large values of $p$. The exact thresholds for the loss of stability depend on both the variable and parameter values and cannot be determined analytically; however, numerical simulation reveals that in the parameter ranges we are interested in, $S_0$ is always stable, $S_1$ is always unstable and $S_2$ can be either stable or unstable.

As an exception, there is one case in which a steady state and stability can be determined analytically: when $\alpha_1$ is zero. We can see from the nullclines that if $\alpha_1$ is zero (i.e. there is no background pro-inflammatory cytokine production), then there is a steady state at $(p, a) = (0, 0)$. Examining the trace and determinant in this case gives $\mathrm{Trace}\,A = -\gamma - 1$, which will always be negative and $\mathrm{Det}\,A = \gamma$, which will always be positive, meaning that the steady state must be stable.